Biomacromolecules

Article

pubs.acs.org/Biomac

Functionalization of Ultrabithorax Materials with Vascular Endothelial Growth Factor Enhances Angiogenic Activity

David W. Howell,[†] Camille L. Duran,[†] Shang-Pu Tsai,[†] Sarah E. Bondos,*[,†,‡] and Kayla J. Bayless*[,†]

[†]Department of Molecular and Cellular Medicine, Texas A&M University Health Science Center, College Station, Texas 77843, United States

[‡]Department of Biochemistry and Cell Biology, Rice University, Houston, Texas 77005, United States

Supporting Information

ABSTRACT: Successful design of tissue engineering scaffolds must include the ability to stimulate vascular development by incorporating angiogenic growth factors. Current approaches can allow diffusion of growth factors, incorporate active factors randomly, or can leave residual toxins. We addressed these problems by genetically fusing the gene encoding Vascular Endothelial Growth Factor (VEGF) with the Ultrabithorax (Ubx) gene to produce fusion proteins capable of self-assembly into materials. We demonstrate that VEGF-Ubx materials enhance human endothelial cell migration, prolong cell survival, and dose-dependently activate the VEGF signaling pathway. VEGF-Ubx fibers attract outgrowing sprouts in an aortic ring assay and induce vessel formation in a chicken embryo chorioallantoic membrane (CAM) assay. Collectively, these results demonstrate that the activity of VEGF remains intact in Ubx materials. This approach could provide an inexpensive and facile mechanism to stimulate and pattern angiogenesis.

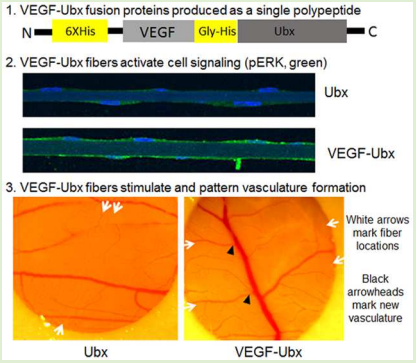

INTRODUCTION

The development of artificial tissues and organs requires scaffolds to support growth of tissue-specific cells, as well as ingrowth of blood vessels within the scaffold to supply those cells with oxygen and nutrients.[1−3] Current difficulties building hierarchical vascular networks confine cell viability in scaffolds to within a few hundred micrometers of the tissue periphery.[4−10] Rapid formation of blood vessels, via neovascularization or angiogenesis, is critical to maintain cell viability within larger tissue engineered scaffolds. Consequently, successful scaffold design should include a strategy to vascularize the tissue.

Scaffold perfusion can be achieved by administering angiogenic proteins, which drive neovascularization in vivo.[11−13] In particular, vascular endothelial growth factor (VEGF) promotes the formation of new blood vessels and can trigger endothelial cell (EC) proliferation, migration, and survival through activation of downstream kinases such as Protein Kinase B (Akt), p38, p44/42 Mitogen Activated Protein Kinases (ERK), and Focal Adhesion Kinase.[14−18] Specifically, VEGF induces EC migration through the ERK pathway.[19−21] Although various strategies have been devised to deliver pro-angiogenic growth factors, an effective system to more precisely direct vascularization of thick scaffolds (>1 mm[4−10]) is still needed. Methods such as microsphere encapsulation,[22] hydrogel entrapment,[23,24] and biospraying technologies[25] effectively provide ECs with pro-angiogenic factors to stimulate formation of capillary networks. Loss of these factors through diffusion may alter cell behavior in neighboring tissues and quickly reduce growth factor efficacy within the scaffold. An alternate approach is to covalently cross-link the functional proteins to the materials. However, cross-linking agents can also inactivate the tethered protein or remain embedded in the materials, rendering them toxic to cells.[26,27] Additionally, the cross-linking strategy can orient some portion of the protein such that ligand binding, and hence protein function, is blocked.[28] While all of these methods show great promise in vitro, they have limited use for building vascular networks in thick tissue scaffolds that require patterns of vascular and nonvascular cells, because pro-angiogenic factors are randomly distributed throughout the scaffold.[10,29−34] Thus, successfully engineered scaffolds must not only present and pattern active stimulatory factors, but also do so using nontoxic methods.

Therefore, we tested whether gene fusion, a new method of delivering growth factors, can successfully stimulate blood vessel growth in tissue engineered scaffolds. Our lab has developed materials composed of the *Drosophila melanogaster* Hox protein Ultrabithorax (Ubx), which self-assembles rapidly in mild, aqueous buffers into fibers, films, and sheets. The amino acid sequence of VEGF monomers can be incorporated into Ubx materials via gene fusion.[35,36] In this approach, the gene encoding a functional protein is fused to the *ubx* gene without intervening stop codons. As a result, a single polypeptide is produced containing the amino acid sequences of both the functional protein and Ubx. Gene fusion provides

Received: July 14, 2016
Revised: October 6, 2016
Published: October 7, 2016

DOI: 10.1021/acs.biomac.6b01068
Biomacromolecules 2016, 17, 3558−3569

unique advantages over other functionalization methods. First, the functional protein is produced as a component of the materials, and thus does not need to be separately produced or purchased and subsequently incorporated into the materials. This single-pot synthesis of materials represents a substantial savings of cost and effort. Second, since the point of attachment is uniform, all molecules of the functional protein in the materials should be similarly oriented and thus equally active. Finally, all Ubx proteins carry a functional protein in the materials, providing a high level of incorporation while preventing the uneven distribution that is often a consequence of chemical cross-linking.[37]

Successfully creating functionalized materials via gene fusion requires overcoming two specific challenges. First, the addition of the functional protein cannot prevent the production or assembly of the resulting fusion protein. Previously, we created VEGF-Ubx and Enhanced Green Fluorescent Protein-VEGF-Ubx (EGFP-VEGF-Ubx) fusions. There was a special concern that these fusions would fail to form materials, because native VEGF is a dimer, and dimerization induced by the VEGF components had the potential to misposition Ubx and preclude assembly. However, both VEGF-Ubx and EGFP-VEGF-Ubx fusions self-assembled to form fibers, and the appended proteins had no significant effect on yield, as measured by fiber length.[36]

The second challenge is for the appended protein to retain activity once embedded in the materials. This step is particularly problematic because (i) protein-based materials are often assembled under conditions that unfold and inactivate most proteins and (ii) the assembly of the materials could sterically conflict with and, thus, unfold the appended protein. Multiple laboratories have used gene fusion to incorporate small peptides and proteins that function in an unstructured state, and thus are not subject to these problems.[38−41] We have previously fused small, stable, structured monomeric proteins to Ubx that retain activity in the chimeric materials.[35] For proteins that bind ligands, the protein must be oriented such that the ligand has access to the binding site. Previously tested Ubx fusion proteins bound small, diffusible molecules (e.g., O_2 binding myoglobin) and thus orientation was not a factor. The Hedhammar group took this approach a step further, and used gene fusion to incorporate into silk-based materials small, single domain proteins that function by binding other proteins, an activity which is expected to be dependent on protein orientation.[38,42] Finally, some proteins must oligomerize to function. However, materials assembly could favor dissociation of these proteins into inactive monomers. Thus far, the only proteins proven to retain activity are small, stable, soluble, and single domain monomers.[35,36,39−42] Protein materials functionalized through gene fusion have not previously demonstrated incorporation of active dimers.

Genetically fusing growth factors or cytokines to incorporate them into materials is potentially challenging, because these proteins are frequently dimers.[43−46] In addition, growth factors and cytokines are often unstable, providing a mechanism to turn off signaling via loss of protein structure/function.[47−50] Finally, both dimerization and the requirement to bind receptors on the cell surface further restrict the range of orientations in which the appended growth factor can be active.[51,52]

In this study we used VEGF-Ubx and EGFP-VEGF-Ubx fusion fibers (Figure S1, Supporting Information) to test the activity of complex protein fusions in Ubx fibers using in vitro, ex vivo, and in vivo assays. Like many growth factors, VEGF is a dimer, is unstable, and has poor solubility.[36] This approach provides a novel method for delivering stable VEGF (Figure S2, Supporting Information) to activate and promote survival of ECs in a dose-dependent manner. Furthermore, when VEGF-Ubx fibers are embedded in collagen matrices, they can selectively influence only the sprouting ECs that intersect with the fiber, effectively immobilizing active VEGF within the composite material. Since VEGF is only located on Ubx materials, and we can place these fibers within 3D collagen matrices, we are effectively controlling the location of VEGF in the experiment. Finally, by fusing VEGF to Ubx, we can direct vascular growth in vivo in a CAM assay with VEGF-Ubx materials. Thus, Ubx is a unique, biocompatible material[53,54] able to incorporate an active growth factor with tunable mechanical properties.[55−57] To our knowledge, this is the first reported study to append VEGF to biomaterials via gene fusion.

2. EXPERIMENTAL SECTION

2.1. Ubx Materials. Monomers of his-tagged Ultrabithorax splicing isoform Ia, along with enhanced GFP (EGFP), VEGF, and EGFP-VEGF Ubx,[36] were produced in *E. coli* as previously described.[53] DNA sequences encoding all protein fusions were inserted into the NdeI site of pET19b-Ubx, between the N-terminal His-tag and Ubx before transformation into Rosetta (DE3) pLysS cells (Novagen). Overnight liquid cultures were inoculated from single colonies. Protein expression was induced at mid log phase with 1 mM isopropyl-β-D-1-thiogalactopyranoside (IPTG) for 4 h and cells were harvested by centrifugation and stored at −20 °C. Pellets were lysed and cell debris was removed by centrifugation for 30 min at 17000 rpm. Ubx protein was purified from the clarified cell lysate by nickel-nitrilotriacetic acid chromatography (Thermo). Fibers, pulled from films produced in a "buffer reservoir"[35] containing 50 mM sodium phosphate, 500 mM NaCl, and 5% glucose w/v, at pH 8.0, were wrapped around a 5 mm sterile plastic inoculation loop and stored in a sterile tissue culture dish until use. Although green fluorescent fibers could not be used for experiments monitored by immunofluorescence, EGFP-Ubx and EGFP-VEGF-Ubx were used for all other experiments to (i) increase expression of the monomers in *E. coli* and (ii) visualize the fibers using green fluorescence. The presence of EGFP does not alter the assembly of Ubx or VEGF-Ubx materials.[36] The EGFP-fused constructs could not be used in immunoassays in which green fluorescence is one of the reporters.

2.2. Cell Culture. Primary human umbilical vein endothelial cells (Lonza, C2517A) were cultured and used at passages 3−6. Cells were grown on gelatin-coated tissue culture flasks, passaged once per week in M199 growth medium supplemented with heparin, bovine hypothalamic extract, 10% fetal bovine serum, antibiotics, and gentamycin as described.[58] For experiments monitoring total and phosphorylated levels of ERK or VEGFR2, endothelial cells (ECs) were seeded onto fibers and cultured overnight. The composition of the fibers varied for each experiment, and is detailed in the relevant Results and Discussion section. Cell culture growth media was replaced with basal media without serum for 0−4 h, as indicated, prior to assessing protein concentration using immunofluorescence or Western blotting as described below.

2.3. Immunofluorescence. Cell suspensions were incubated with Ubx fibers with diameters ranging from 7 to 10 μm, wrapped 2−4 times around inoculation loops to allow cells to attach to fibers and cultured as previously described.[53,54] For time course experiments, cells cultured on Ubx were transferred to new wells containing M199 without serum for 0 to 4 h. While ECs seeded on VEGF-Ubx were untreated, 40 ng/mL of soluble VEGF in 1 mL of media was added to ECs seeded on Ubx alone to compare cell responses to immobilized versus soluble VEGF. In all immunofluorescence experiments, 500 μL of a freshly made 10% paraformaldehyde solution in PBS (16 mM Na_2HPO_4, 2.6 mM KCl, 1.2 mM K_2HPO_4, 68 mM NaCl) was added to the existing culture media yielding a final concentration of 4%, and

DOI: 10.1021/acs.biomac.6b01068
Biomacromolecules 2016, 17, 3558−3569

samples were fixed prior to two 15 min washes with a 25 mM Tris, 200 mM glycine solution. Samples were then permeabilized with 500 μL of 0.5% Triton X-100 solution in PBS for 20 min. Wells were aspirated and samples were blocked overnight in 500 μL of blocking solution (0.1% Triton X-100, 1% BSA, 0.2% sodium azide, and 5% goat serum) at 4 °C. Primary antibodies raised against ERK (1:100; Cell Signaling Technology), and pERK (phosphorylated at T202/Y204; 1:1000; Cell Signaling Technology) were diluted in blocking solution and incubated in the wells for 3 h. Primary antibodies against VEGFR2 (1:300; Abcam) were used on samples without the permeabilization step, and the blocking buffer in these experiments lacked Triton X-100. Loops were washed three times for 10 min each in 0.1% Triton X-100 in PBS (500 μL) and incubated with goat antirabbit Alexa Fluor 488 and goat antimouse Alexa Fluor 594 conjugated secondary antibodies (both 1:200; Molecular Probes) in blocking solution for 1 h. Loops were washed three times and counterstained with 10 mM 4′,6-diamidino-2-phenylindole (DAPI; Molecular Probes), placed on a 22 mm × 55 mm coverslip, and imaged immediately using confocal microscopy on a Nikon Eclipse Ti equipped with NIS Elements AR 4.10.01 software.

2.4. Migration Assay. DiI-labeled HUVECs[53,54] were seeded onto gelatin-coated wells and allowed to reach confluency. Cells were then cultured in M199 without serum for 6 h prior to placement of inoculation loops wrapped with EGFP-Ubx or EGFP-VEGF-Ubx fibers onto cell monolayers. After a 16 h incubation in M199 with 1.5% serum, the cells on Ubx fibers were fixed and immunofluorescence was conducted as described above.

2.5. Terminal Deoxynucleotidyl Transferase dUTP Nick End Labeling (TUNEL) Assay. Fiber-wrapped loops, directly seeded with 35000 cells suspended in 250 μL of growth media, were cultured overnight so that cells could attach to Ubx fibers. Growth medium was aspirated, and cells cultured on Ubx fibers were starved for 8 h in M199 without serum and then fixed using paraformaldehyde. A TUNEL assay kit from Abcam was used per manufacturers' protocol and imaged using confocal microscopy, as described above.

2.6. Western Blot. Loops containing attached cells were collected in 60 μL of preheated Laemmli sample buffer and boiled in microcentrifuge tubes for 10 min at 95 °C. Protein lysates were separated by SDS-PAGE and transferred to polyvinylidene fluoride membranes (Fisher Scientific). After blocking in 5% nonfat dry milk or BSA at room temperature for 1 h, the membranes were incubated with monoclonal antisera directed against PECAM (1:1000 in tris-buffered saline with 0.1% Tween 20 (TBST); Cell Signaling Technology), ERK (1:1000 in TBST; Cell Signaling Technology), pERK (1:1000 in TBST; Cell Signaling Technology), GAPDH (1:10,000 in TBST; Abcam), VEGFR2 (1:750 in TBST; Abcam), and pVEGFR2 (1:750 in TBST; Life Technologies) at room temperature for 3 h. The membranes were washed three times before incubation with rabbit antimouse secondary antibody or goat antirabbit secondary antibody (1:5000; DAKO) for 1 h. Immunoreactive proteins were visualized using enhanced chemiluminescence (Millipore) followed by exposure to film (Denville Scientific). For image quantification, images were scanned with a FluorChem 8900 digital imaging system (Alpha Innotech, San Leandro, CA). Band intensities were measured using NIH ImageJ image analysis software. Western blots analyzing ERK and pERK were probed on separate gels. PECAM is robustly expressed on ECs, and remains relatively constant with time allowing it to be used as a control for the amount of sample loaded for both gels.[59,60] For quantification of ERK/pERK ratios, the intensities of ERK and pERK bands were normalized to PECAM prior to comparison with each other.

2.7. Aortic Ring Assay. Aortae were harvested from Sv129-Pas mice between 6 and 10 weeks of age and prepared as described.[61] Aortae were cut into 0.5 mm segments along the length of the vessel, creating rings. Collagen type I was prepared at a concentration of 1.5 mg/mL, as previously described,[58] substituting Opti-MEM (Gibco) for M199. Collagen (150 μL) was added to each well of a 48-well, glass bottom plates (MatTek) on ice. One aortic ring per well was embedded in the collagen. Prior to collagen polymerization, loops wrapped with EGFP-Ubx or EGFP-VEGF-Ubx fibers were placed in the collagen so that the fibers were in close proximity (within 50 to 500 μm) of the aortic ring to allow for outgrowing sprouts to intersect and physically contact fibers during the 6 day assay. After the collagen polymerized, 500 μL of Opti-MEM containing 2.5% FBS, gentamycin, and 40 ng/mL VEGF was added. Rings were incubated at 37 °C with 5% CO_2. After 24 h, VEGF-containing media was removed and replaced with media lacking VEGF. After six total days of incubation, samples were fixed with 4% paraformaldehyde in PBS for 30 min. Wells were rinsed two times for 30 min with Tris-Glycine buffer (0.3% Tris and 1.5% Glycine). After rinsing, samples were permeabilized with 0.5% Triton X-100 in PBS by rocking for 2 h at room temperature and then blocked overnight with 0.1% Triton X-100, 1% BSA and 1% goat serum in Tris-buffered saline at room temperature. Samples were incubated at room temperature with gentle agitation for 3 h in solutions containing primary antibodies directed against PECAM-1 (BD Transduction, 550274) diluted 1:100 in blocking buffer. After washing four times for 30 min with 1 mL 0.1% Triton X-100 in PBS at room temperature, samples were incubated with Alexa Fluor 595-conjugated secondary antibodies (Molecular Probes) diluted 1:200 in blocking buffer at 4 °C overnight. The samples were then washed overnight at room temperature with 1 mL of 0.1% Triton X-100 in PBS. Nuclei were stained with 1 μM DAPI (Molecular Probes) for 30 min at room temperature with gentle agitation and imaged as described above. Z-stack images (5−25 μm) were taken using 0.5 μm steps, compressed, and analyzed using Nikon Elements Software. While blinded, the percent of sprouts that followed the fiber was quantified by dividing the number of sprouts which followed fibers by the total number of fiber−sprout interactions. For example, a single fiber encountering three vessels was analyzed as three data points in this analysis.

2.8. Chorioallantoic Membrane Assay (CAM). Fertilized eggs were obtained from the Texas A&M University Poultry Science Center (College Station, TX). Eggs were incubated at 37 °C, rotating continuously for 3 days before ex ovo culture.[62−64] Eggs were wiped with betadine and cracked into sterile weigh boats (VWR) containing penicillin (100 internal unit/mL) and streptomycin (100 μg/mL; Gibco), fungizone (1 μg/mL; Sigma), niacin (500 ng/mL; Sigma), and gentamicin (50 μg/mL; Gibco) based on an average volume of 60 mL/egg. Embryos were covered and placed in a humidified incubator (37 °C) for 4 days. Ubx materials were wrapped around 15 × 15 mm sterile blot paper with 8 mm holes punched in the center. Fibers were placed perpendicular to established vessels. On the same day Ubx materials were added, micrographs were captured using a National dissection scope (Model DC5−420TH). Following imaging, embryos were cultured for 48 h. The embryos were then sacrificed and the same field was imaged to assess development of new vessels along Ubx fibers. To visualize fibers and the vessel boundaries, images were also captured using illumination with UV light. Vessel growth was quantified by comparing the images before and after addition of Ubx materials and counting the number of new vessels established along fibers.

RESULTS AND DISCUSSION

Human Endothelial Cells Signal through the ERK Pathway When Presented with VEGF on Ubx Materials. A challenge in creating functionalized materials from protein chimeras has been assembling the materials while maintaining the structure and activity of the appended functional protein. We have created several active, functionalized materials using the self-assembling protein Ubx as a platform to introduce new activities via formation of protein fusions.[36] However, thus far, only stable, monomeric proteins have been shown to retain activity in Ubx materials. To use Ubx as a vascular scaffold, proangiogenic proteins such as VEGF, which is significantly less soluble and dimeric, must be appended so that the materials can interact with and direct vascular cells. VEGF is present in high concentrations during materials assembly, where low solubility could cause VEGF-Ubx to form inactive aggregates.

DOI: 10.1021/acs.biomac.6b01068
Biomacromolecules 2016, 17, 3558−3569

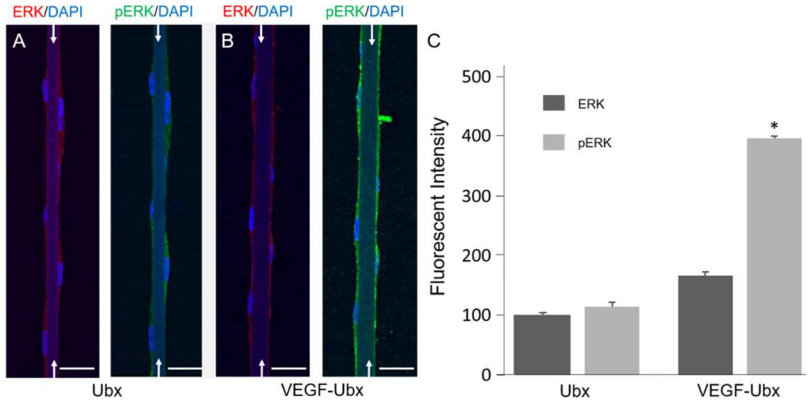

Figure 1. Endothelial cells cultured on VEGF-Ubx fibers show significantly greater phosphorylation of ERK. ECs seeded on (A) Ubx fibers and (B) VEGF-Ubx fibers were cultured overnight and then starved for 2 h prior to fixation in 4% paraformaldehyde. Fibers in all panels are indicated by white arrows. Cells were stained for ERK (red), pERK (T202/Y204) (green), and counterstained with DAPI (a blue fluorescent stain that binds DNA) for immunofluorescence imaging using confocal microscopy. Scale bars = 20 μm. (C) Quantification of fluorescent intensity of ERK and pERK signal intensity. Data are representative of 3 experiments with 6 replicates and averaged from 25 independent fields in each group (±SEM) with analysis for significance using univariate analysis of variance (ANOVA) with Tukey's honest significant differences (HSD) test posthoc. Note that ECs cultured on VEGF-Ubx exhibit higher pERK staining compared to Ubx fibers (*p < 0.01), whereas differences in total ERK staining between the two samples were not statistically significant (p < 0.06).

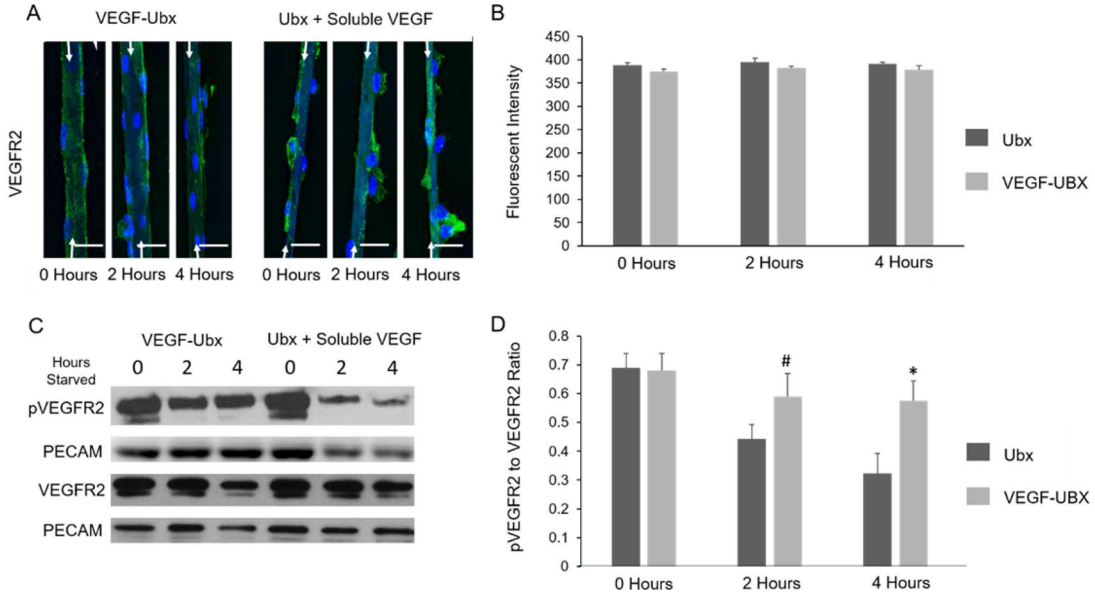

Figure 2. VEGFR2 cell surface expression is unchanged, while phosphorylation is sustained by VEGF-Ubx. (A) Immunofluorescence staining for VEGFR2 surface expression in nonpermealized ECs (green) counter stained with DAPI (blue) on VEGF-Ubx or Ubx fibers (white arrows). Cells were seeded overnight on the materials indicated. Growth medium was removed and replaced with M199 alone (VEGF-Ubx) or M199 + 40 ng/mL soluble VEGF (Ubx + soluble VEGF). Cells were fixed at 0, 2, and 4 h and stained. Scale bars = 20 μm. (B) Quantification of VEGFR2 fluorescence in the absence of permeabilization using antibodies against the extracellular motif in VEGFR2. (C) ECs seeded onto EGFP-Ubx and EGFP-VEGF-Ubx fibers were cultured overnight and then serum starved for 0−4 h. ECs cultured on Ubx fibers were treated with 40 ng/mL soluble VEGF at onset of starvation. Cells were collected, lysed, and analyzed using Western blot analysis. Membranes were probed for pVEGFR2 (Tyr 1214), VEGFR2, and the loading control PECAM. (D) Ratio of pVEGFR2/VEGFR2 signal intensity following normalization to PECAM loading controls. Data were averaged from five experiments and analyzed for significance using univariate analysis of variance (ANOVA) with Tukey's honest significant differences (HSD) test posthoc with # indicating p < 0.02 vs GFP-Ubx at 2 h and * indicating p < 0.01 for EGFP-VEGF-Ubx vs GFP-Ubx at 4 h.

Furthermore, the geometry and spacing imposed on VEGF monomers by Ubx packing in the material could prevent formation of active VEGF dimers. To test if VEGF immobilized in Ubx fibers is active, Ubx or VEGF-Ubx fibers bound to endothelial cells (ECs) were transferred to basal media without serum for 2 h to reduce stimulation from the growth media, and probed for VEGF activity (Figure 1A,B). During angiogenesis, VEGF signaling stimulates ERK phosphorylation downstream of VEGFR2.[65−74] While total ERK levels are unchanged in all samples, pERK is significantly greater for cells cultured on VEGF-Ubx fibers than for cells cultured on unmodified Ubx fibers (Figure 1C). This indicates that ERK is activated in ECs when presented with VEGF genetically fused to Ubx materials.

Signaling through VEGFR2 by VEGF-Ubx Fibers Is Sustained for Longer Times Relative to Soluble VEGF. A variety of cell signaling receptors signal via ERK. To verify that

DOI: 10.1021/acs.biomac.6b01068
Biomacromolecules 2016, 17, 3558−3569

VEGF fused to Ubx fibers is signaling through the correct pathway, we also tested whether the VEGF receptor VEGFR2 is activated, and thus phosphorylated. At the cellular level, VEGF binding to VEGFR2 results in Ca^{2+} mobilization, prostacyclin production, nitric oxide production, and phosphatidylinositol-3-kinase (PI3K)/Akt activation, in addition to ERK activation.[75−78] These events cumulatively stimulate EC proliferation and migration, behaviors required for an angiogenic response.[75−78] We first verified that VEGF-Ubx leads to VEGFR2 activation and thus has the potential to instigate all of these events. To compare the effects of soluble VEGF stimulation on VEGF-Ubx versus unmodified Ubx fibers, ECs cultured only on the control Ubx fibers were treated with physiologically relevant[14,58,63,73,79−81] concentrations of soluble VEGF at the onset of serum starvation. Staining unpermeabilized cells revealed that VEGFR2 surface presentation is unchanged and therefore any changes in receptor phosphorylation during the course of these experiments are not a result of VEGFR2 internalization or downregulation.

The extent of VEGFR2 phosphorylation (pVEGFR2) was quantified by Western blot analysis (Figure 2C). High levels of pVEGFR2 are observed in serum-starved cells either cultured on VEGF-Ubx fibers or on unmodified Ubx fibers in the presence of soluble VEGF at time 0, while VEGFR2 phosphorylation is sustained at significantly higher levels on VEGF-Ubx at 2 and 4 h following serum withdrawal. In contrast, VEGFR2 phosphorylation declines in ECs seeded on Ubx and treated with soluble VEGF at 2 and 4 h following serum withdrawal (Figure 2D). PECAM loading controls remained relatively constant with time in all groups. Therefore, when VEGF is immobilized on Ubx materials via gene fusion, it is not only able to activate its receptor, but also to maintain VEGFR2 activation for a longer period of time than soluble VEGF.

Although the VEGFR2 receptor is activated, the orientation or immobilization of VEGF on Ubx materials could force an unusual VEGF:VEGFR2 interaction interface that prevents activation of downstream signaling pathway components by VEGFR2. If ERK is directly activated by VEGFR2 on VEGF-Ubx materials, then the duration of ERK phosphorylation is expected to match the duration of VEGFR2 phosphorylation (4 h). In contrast, if ERK activation is mediated by residual soluble VEGF or if VEGF is proteolyzed from the materials, then ERK should be activated transiently, for no more than 1 h.[82,83] To distinguish these possibilities, the duration of signaling by immobilized versus soluble VEGF was measured for fiber bound ECs after exposure to starvation conditions. Because activation was monitored by Western blot instead of immunofluorescence, EGFP-Ubx and EGFP-VEGF-Ubx could be used in these experiments to (i) increase expression of the monomers in *E. coli*[36] and (ii) visualize the fibers using green fluorescence. Cell lysates from each group were collected every hour for Western blot analysis of ERK phosphorylation (Figure 3A,B). The ratio of pERK to ERK signaling intensities, normalized to PECAM loading controls, shows that ERK activation in ECs cultured on EGFP-VEGF-Ubx fibers can be sustained for at least 4 h, while ERK activation almost completely disappears on EGFP-Ubx materials treated with soluble VEGF within 1 h (Figure 3C). Thus, EC interactions with EGFP-VEGF-Ubx fibers result in sustained ERK signaling when compared to EGFP-Ubx materials treated with soluble VEGF. After 4 h, the observed decrease in VEGF signaling could be caused by depletion of available downstream proteins

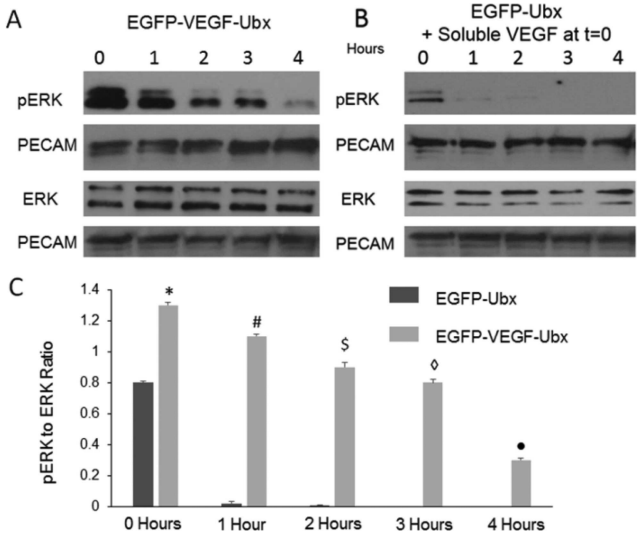

Figure 3. VEGF-Ubx materials sustain ERK signaling in ECs. ECs seeded onto (A) EGFP-VEGF-Ubx and (B) EGFP-Ubx fibers were cultured overnight and then starved for 4 h. ECs cultured on EGFP-Ubx were treated with 40 ng/mL soluble VEGF at the onset of starvation. Cells were collected at the specified time, and Western blot analyses were used to probe for pERK (Thr 202/Tyr 204), ERK, and PECAM. (C) Ratio of pERK/ERK signal intensities normalized to PECAM loading controls. Data were averaged from four experiments and analyzed for significance using univariate analysis of variance (ANOVA) with Tukey's honest significant differences (HSD) test posthoc with * indicating $p < 0.01$ vs EGFP-Ubx at 0 h, # indicating $p < 0.03$ vs EGFP-VEGF-Ubx at 1 h, $ indicating $p < 0.04$ vs EGFP-VEGF-Ubx at 2 h, ◊ indicating $p < 0.05$ vs EGFP-VEGF-Ubx at 3 h, and ● indicating $p < 0.01$ vs EGFP-VEGF-Ubx at 4 h.

due to continuous signaling or by proteolysis of VEGF from the fiber. However, when cells are cultured on EGFP-VEGF-Ubx fibers for 24 h, the EGFP signal is retained (Figure S2, Supporting Information). Since VEGF links EGFP to the fiber, VEGF must still be present as well. Rapid, yet transient increases in ERK and VEGFR2 phosphorylation in response to soluble VEGF are in agreement with other studies.[34,84−87] VEGF signaling through VEGFR2 can result in receptor internalization and degradation of the VEGF/VEGFR2 complex,[88] although Anderson et al. showed that internalization is not required for VEGF signaling.[84,85] Multiple laboratories are testing various methods, such as 3D printing[34,89,90] to immobilize VEGF,[91,92] prevent diffusion,[93] and allow for complex patterning.[29,33,34] Not only does covalently immobilizing VEGF induce signaling and enhance cell activity,[30,87] it also promotes vessel formation.[86,94−96] The ability of VEGF-Ubx materials to elicit signaling through ERK and VEGFR2 phosphorylation is similar to other studies in which VEGF is covalently attached to materials.[34,84,85] However, no study reports signal duration of longer than 1 h. It is unclear if this is a failure of other methods or simply a lack of investigation beyond 1 h. Here, VEGF appended to Ubx sustains signaling for over 4 h, demonstrating that this method of functionalizing materials with VEGF is unique. In addition, the robustness of this approach is demonstrated by the fact that VEGF is active when incorporated into both VEGF-Ubx and EGFP-VEGF-Ubx materials.

VEGF Signaling Is Proportional to VEGF Concentration on Fibers. EC responses to VEGF in vitro are dependent on exposure to adequate concentrations of VEGF,[79]

DOI: 10.1021/acs.biomac.6b01068
Biomacromolecules 2016, 17, 3558−3569

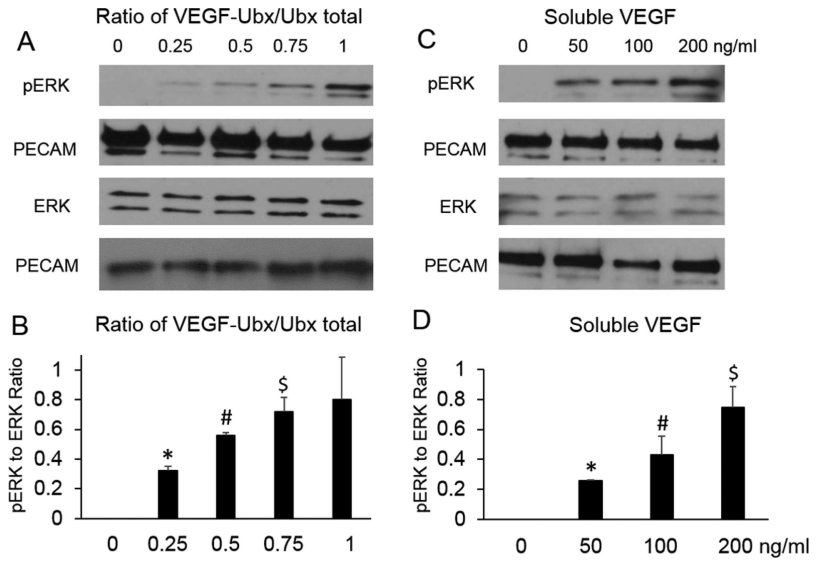

Figure 4. ERK phosphorylation is proportional to the amount of VEGF incorporated into Ubx materials. (A) ECs seeded onto fibers composed of an increasing ratio of VEGF-Ubx to Ubx fibers were cultured overnight and then starved for 2 h prior to lysis in sample buffer and Western blot analysis. Membranes were probed for pERK (Thr202/Tyr204), ERK, and PECAM. (B) ERK and pERK band intensities were normalized to PECAM loading controls from respective blots. The ratio of PECAM-normalized pERK/ERK was averaged from four experiments and analyzed for significance using univariate analysis of variance (ANOVA) with Tukey's honest significant differences (HSD) test posthoc with * indicating $p < 0.01$ vs 0 VEGF-Ubx, # indicating $p < 0.02$ vs 0.25 VEGF-Ubx to total Ubx, and $ indicating $p < 0.04$ vs 0.5 VEGF-Ubx to total Ubx. (C) ECs seeded onto Ubx fibers were cultured overnight and then starved for 2 h prior to treatment with increasing concentrations of soluble VEGF. After 30 min of treatment, cell lysates were analyzed by Western blotting and probed for pERK, ERK, and PECAM. (D) Quantification of PECAM-normalized pERK to ERK ratios were performed as in (B). Data were averaged from four experiments and analyzed for significance using univariate analysis of variance (ANOVA) with Tukey's honest significant differences (HSD) test posthoc with * indicating $p < 0.02$ vs 0 ng/mL, # indicating $p < 0.03$ vs 50 ng/mL, and $ indicating $p < 0.01$ vs 100 ng/mL.

while in vivo, overexpression of VEGF can result in aberrant angiogenesis[97] and enhanced angiogenic responses within tumors.[98−101] If VEGF in Ubx materials is only partially active, the material may not reach the threshold necessary to elicit a cellular response. Alternately, because the VEGF sequence is appended to every Ubx protein, the VEGF concentration could be too high and thus overstimulate cells. Therefore, to elicit the appropriate cellular responses for in vivo vascular scaffolds, it is important to present an effective concentration of active VEGF on Ubx materials. Previously, we established that the ratio of Ubx to EGFP-Ubx produces materials in which EGFP-Ubx content in fibers linearly correlates with the percentage of EGFP-Ubx monomers in the original protein mixture.[36] We used this approach to generate fibers with varying VEGF concentrations. ECs were cultured on Ubx materials made from increasing ratios of VEGF-Ubx to Ubx (Figure 4), then serum starved and probed for ERK phosphorylation. Expression of total ERK remained constant while levels of pERK increased proportionally with VEGF concentration, up to a 0.75 ratio of VEGF-Ubx to total Ubx (Figure 4A,B). This VEGF concentration-dependent increase in ERK phosphorylation provides further evidence that immobilized VEGF is the active agent. Above a ratio of 0.75 VEGF-Ubx to total Ubx, the response began to plateau.

Because ERK phosphorylation is linearly proportional to VEGF-Ubx concentrations, we can infer that appending VEGF to Ubx does not interfere with materials assembly. To benchmark the extent of signaling elicited by VEGF incorporated into Ubx fibers with signaling elicited by soluble VEGF monomers, we administered increasing doses of soluble VEGF to ECs cultured on Ubx fibers and monitored pERK/ERK ratios (Figure 4C,D). The level of pERK/ERK observed with the physiological concentration of 50 ng/mL soluble VEGF[14,58,63,73,79−81] was similar to the pERK/ERK level induced by materials containing a ratio of 0.25 VEGF-Ubx to total Ubx. Therefore, Ubx materials are likely to be useful for building in vivo vascular scaffolds because a broad range of VEGF concentrations can be incorporated into Ubx fibers and, more importantly, can present VEGF at levels that elicit comparable signals to physiological doses of soluble VEGF. Furthermore, because only 25% of the monomers need to be functionalized with VEGF, space is available for incorporating additional angiogenic molecules.

VEGF-Ubx Promotes Endothelial Cell Migration and Survival In Vitro. VEGF impacts many signaling cascades to elicit a variety of cell behaviors.[14−18] Therefore, the ability of VEGF-Ubx fibers to phosphorylate ERK via VEGFR2 activation does not guarantee the entire repertoire of VEGF functions will be activated by immobilized VEGF. We tested whether complex cell behaviors, normally regulated by soluble VEGF, can be elicited by VEGF-Ubx fibers. In particular, we asked whether VEGF signaling can induce cells to migrate in low serum conditions or prevent cells from undergoing apoptosis in growth factor-depleted media. In migration assays, a confluent monolayer of ECs labeled with DiI, a red fluorescent lipophilic dye, were cultured in low serum prior to the addition of Ubx fibers. Cells that contact fibers and bind active VEGF are expected to migrate onto the fiber (Figure 5A,B). A significantly greater number of cells migrated onto EGFP-VEGF-Ubx fibers when compared to control EGFP-Ubx fibers (Figure 5C), indicating that VEGF-Ubx materials stimulated migration of ECs in low serum conditions, while EGFP-Ubx materials did not.

DOI: 10.1021/acs.biomac.6b01068
Biomacromolecules 2016, 17, 3558−3569

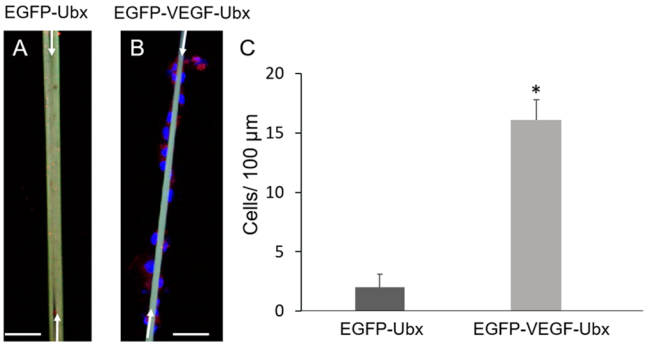

Figure 5. EGFP-VEGF-Ubx fibers promote enhanced recruitment and migration of endothelial cells. EGFP-Ubx (A) and EGFP-VEGF-Ubx (B) fibers (green, labeled with white arrows) were cultured overnight with an established monolayer of DiI-labeled (red) endothelial cells in low (1.5%) serum. Cells were fixed, stained with DAPI (blue), and imaged using confocal microscopy. Scale bars = 50 μm. (C) Quantification of the number of cells/100 μm distance attached to EGFP-Ubx vs EGFP-VEGF-Ubx fibers. Data were averaged from 25 independent fields in each group (±SEM) from four experiments. Data were analyzed for significance using univariate analysis of variance (ANOVA) with Tukey's honest significant differences (HSD) test posthoc with * indicating $p < 0.01$.

In addition to migration, VEGF functions as a survival factor to inhibit apoptosis.[102−104] To test if Ubx materials sustain cell viability under stressful conditions, we cultured an equal number of ECs directly on EGFP-Ubx and EGFP-VEGF-Ubx fibers to allow for cellular attachment prior to serum starvation. While apoptotic (red, TUNEL positive) cells were detected on EGFP-Ubx fibers (Figure 6A), cells that were cultured on EGFP-VEGF-Ubx fibers showed little evidence of apoptosis (Figure 6B). Comparison of the number of cells at Time 0 to the number of cells after 8 h of starvation shows a significantly higher retention rate of ECs on EGFP-VEGF-Ubx materials than EGFP-Ubx (Figure 6C). Furthermore, these data indicate the majority of cells cultured on EGFP-Ubx fibers were lost. The few remaining cells on EGFP-Ubx materials were positive for TUNEL staining, while only 7% of cells remaining on EGFP-VEGF-Ubx fibers were TUNEL positive (Figure 6C). Therefore, EGFP-VEGF-Ubx fibers promote EC migration and survival, which are beneficial behaviors consistent with VEGFR2 and ERK activation shown above.

VEGF-Ubx Materials Recruit Endothelial Sprouts in an Ex Vivo Aortic Ring Assay. An important aspect of VEGF function is to direct angiogenic vessel outgrowth. Therefore, we used the physiologically relevant aortic ring assay to examine how VEGF-Ubx materials might affect vascular tissues. In this assay, angiogenic vessels sprout from freshly isolated aortic tissue that is embedded in a collagen matrix, allowing for analysis of vascular sprouting in an ex vivo environment. This assay is ideal for these experiments because clearly visible, lumenized, capillary-like structures emanate linearly from the tissue at a rate similar to in vivo angiogenic sprouts.[61,105] Although the experiments described above focus on ECs, this assay more closely resembles angiogenic events in vivo because supporting cells, such as smooth muscle cells and pericytes, participate in the formation of microvessels.

To examine Ubx interactions with angiogenic sprouts, we modified the aortic ring assay by placing Ubx fibers within collagen matrices in close proximity to embedded tissue segments to allow for interaction with newly formed outgrowths as sprouts develop (Figure S3, Supporting Information). Normally, sprouts do not deviate from their original linear path. However, when endothelial sprouts intersect EGFP-VEGF-Ubx fibers, the direction sprouts are growing is frequently altered to follow the fibers (Figure 7A,B). In some cases, the sprouts wrap around the fibers (solid arrow heads; Figure S4, Supporting Information). These effects are rarely observed when outgrowing sprouts encounter EGFP-Ubx fibers (open arrowheads, Figure 7C,D and Figure S5, Supporting Information). Quantification of these events demonstrates that outgrowing sprouts change direction at a significantly higher rate when intersecting EGFP-VEGF-Ubx versus EGFP-Ubx (Figure 7E). Because we observe comparable frequencies of initial contact between angiogenic sprouts and EGFP-VEGF-Ubx and EGFP-Ubx fibers, we conclude that angiogenic sprouts are responding to VEGF and the effect is not caused by (i) durotaxis, (ii) differences in the mechanical properties of fibers and the surrounding collagen, or (iii) differences in sprout attachment to Ubx fibers versus collagen due to the surface chemistry of these materials. Importantly, in this assay the VEGF-Ubx fibers buried in collagen form a composite material, in which VEGF-modified Ubx fibers guide angiogenic sprouts without impacting the behavior of cells within the scaffold that are not in contact with the fiber. This ability to recruit

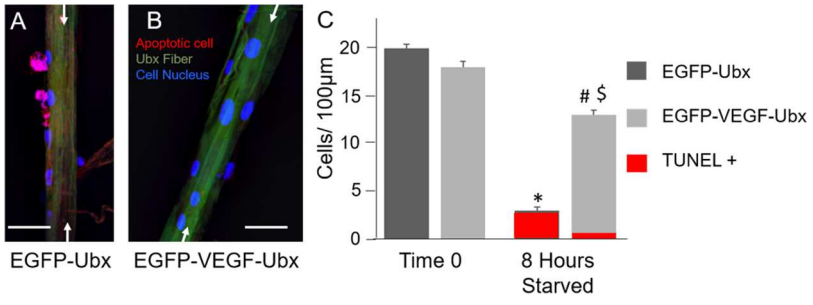

Figure 6. EGFP-VEGF-Ubx fibers prevent endothelial cell apoptosis after starvation. ECs seeded on EGFP-Ubx (A) and EGFP-VEGF-Ubx (B) fibers were starved for 8 h and analyzed using TUNEL assays to detect apoptotic cells. White arrows indicate Ubx fibers. Scale bars = 10 μm. (C) Quantification of the number of viable and TUNEL-positive cells associated with EGFP-Ubx and EGFP-VEGF-Ubx fibers before (time 0) and after 8 h of starvation. Data shown are representative of 5 experiments and averaged from 20 independent fields in each group (± SEM). Statistical significance was determined using univariate analysis of variance (ANOVA) with Tukey's honest significant differences (HSD) test posthoc with * indicating $p < 0.01$ vs time 0, # indicating $p < 0.04$ vs time 0, and $ indicating $p < 0.03$ vs EGFP-Ubx after 8 h starvation. Quantification of TUNEL-positive cells (red) indicated that 95% of cells on EGFP-Ubx and only 7% of cells on EGFP-VEGF-Ubx were TUNEL positive.

DOI: 10.1021/acs.biomac.6b01068
Biomacromolecules 2016, 17, 3558−3569

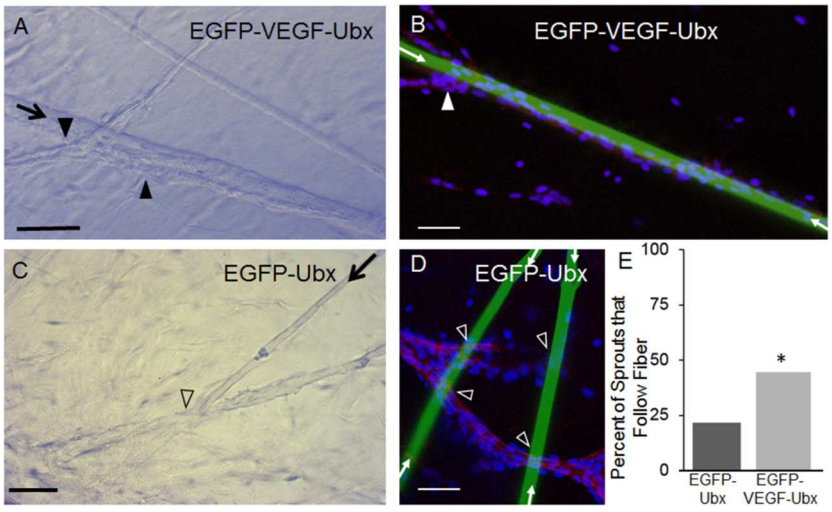

Figure 7. EGFP-VEGF-Ubx materials redirect and attract endothelial positive outgrowths from aortic rings. Aortic vessels excised from mice were divided into 0.5 mm segments and embedded in 3D collagen matrices with Ubx materials (Supporting Information, Figure 3). Aortic rings were cultured for 24 h in VEGF-supplemented media to induce endothelial sprouts into the collagen followed by an additional 5 days in media without growth factors so that EGFP-VEGF-Ubx is the only source of growth factors available to endothelial sprouts. Cultures were fixed, stained for PECAM (red), and counterstained with DAPI (blue). (A) Brightfield and (B) confocal images of EGFP-VEGF-Ubx cultures show that sprouts will alter their direction to follow and in some cases envelop EGFP-VEGF-Ubx fibers (green). Images of EGFP-Ubx cultures using (C) brightfield and (D) confocal imaging. In (A)−(D), scale bars = 50 μm, and black or white arrows indicate EGFP-VEGF-Ubx or EGFP-Ubx materials. Filled arrowheads indicate where sprouts follow fibers, while open arrowheads indicate fibers that interact but do not follow fibers. (E) Quantification of sprout interactions with materials. Data were collected from 50 events in 4 experiments. Values were analyzed for statistical differences using a Chi-Square test for independence with * indicating $p < 0.02$.

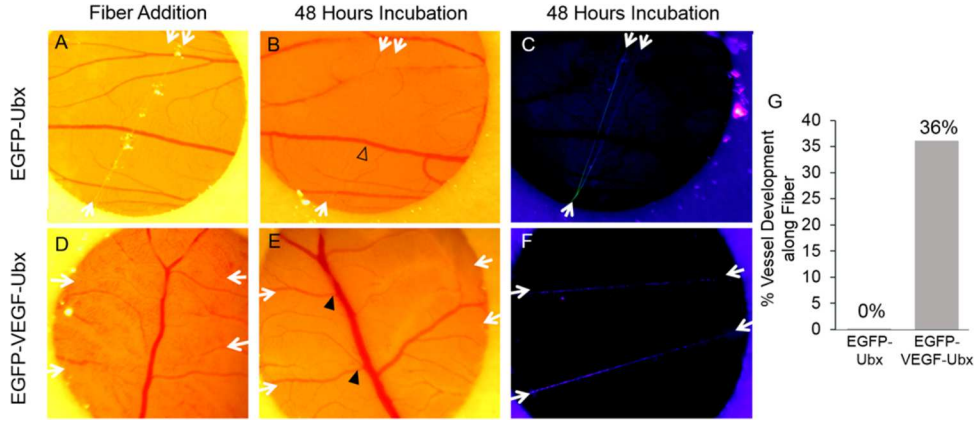

Figure 8. EGFP-VEGF-Ubx fibers elicit more association with vasculature in chicken embryo chorioallantoic membrane (CAM) assays. Fertilized eggs were humidified, rotating continuously for 3 days before ex ovo culture.[62−64] Embryos were cultured for 4 days prior to the addition of (A−C) EGFP-Ubx and (D−F) EGFP-VEGF-Ubx materials placed with fibers perpendicular to established vessels. (A, D) Representative brightfield images of the CAM surface captured immediately after adding materials. (B, E) Brightfield and (C, F) UV-illuminated photographs of the same fields shown in (A) and (D) 48 h later. In (A−F), fiber locations are indicated by white arrows. Open arrowhead indicates absence of vessel development, while filled arrowheads indicate development of new vessels. (G) Quantification of vessel development induced by Ubx materials. The percentage of events where vessels developed in association with materials was quantified for EGFP-Ubx (0/50 events) and EGFP-VEGF-Ubx (18/50 events).

sprouting structures is anticipated to be beneficial when designing tissue engineering scaffolds.

VEGF-Ubx Directs Blood Vessel Formation In Vivo. Thus, far, we have demonstrated that VEGF-fused Ubx fibers can activate the VEGF signaling pathway in cell culture and alter the direction of growth of preformed angiogenic sprouts in the ex vivo aortic ring assay. To test whether EGFP-VEGF-Ubx fibers can also instigate neovascularization in vivo, the ex ovo chicken embryo chorioallantoic membrane (CAM) assay[62−64] was modified for Ubx fibers. In the modified assay, chicken embryos were transferred to cell culture dishes. EGFP-Ubx (Figure 8A) or EGFP-VEGF-Ubx (Figure 8D) fibers placed on the surface of the chorioallantoic membrane of these embryos perpendicular to established vessels were monitored for the formation of new vasculature. New vessels (indicated by filled arrowheads) were observed to form along EGFP-VEGF-Ubx fibers (Figure 8E,F), while vascular development was unaltered by Ubx fibers (open arrowheads, Figure 8B,C). Quantification of 50 events from multiple experiments revealed that 36% of EGFP-VEGF-Ubx fibers placed on the CAM resulted in new vessel growth, while EGFP-Ubx fibers elicited no new vessel growth (Figure 8G). These new vessels grew in the same direction as the VEGF-Ubx fiber axis. Therefore, VEGF-

DOI: 10.1021/acs.biomac.6b01068
Biomacromolecules 2016, 17, 3558−3569

modified Ubx materials can both instigate and direct vascular development in vivo.

CONCLUSIONS

The development of artificial tissues and organs requires scaffolds to physically support growth of tissue-specific cells, as well as blood vessels within the scaffold to supply those cells with oxygen and nutrients.[1−3] In the absence of a functional vasculature, the largest scaffold that can be successfully implanted in vivo is 1−2 mm thick.[4−10] Thus, scaffold construction requires a separate set of molecular cues to direct vascular cell activation, adhesion, proliferation, migration, and maturation. These specific cues must be presented in an active conformation within the scaffold to elicit appropriate cell responses. While great advances have been made, current technologies still have difficulty in adequately and precisely positioning angiogenic factors in a scaffold and maintaining this pattern over time.

As a first step toward this goal, we have demonstrated that VEGF, a dimeric protein, retains activity when genetically fused to Ubx and incorporated into materials. We show that ECs cultured on VEGF-Ubx fibers signal through the appropriate pathway and phosphorylate ERK and VEGFR2. In addition, VEGF signaling is extended for a longer period of time than any other current approach. Our data shows that VEGF concentration in Ubx fibers can be controlled and matched to physiologically relevant concentrations in vitro. Cell culture experiments demonstrate that VEGF-Ubx induces EC migration and sustains cell viability. Angiogenic sprouts change direction when they encounter VEGF-Ubx fibers in an ex vivo aortic ring assay. Finally, in an in vivo CAM assay, VEGF-Ubx fibers induce formation of new vasculature when placed on the surface of the chick chorioallantoic membrane. Collectively, these data demonstrate that Ubx is a unique material able to incorporate active VEGF to direct endothelial cell behavior in vitro and in vivo.

ASSOCIATED CONTENT

Supporting Information

The Supporting Information is available free of charge on the ACS Publications website at DOI: 10.1021/acs.biomac.6b01068.

Schematics of the Ubx fusion proteins used in this paper, analysis of EGFP release from fibers in cell culture, and a schematic of the modified mouse arotic ring assay (PDF).

Z-stack image of an endothelial sprout (blue; DAPI stained cells) wrapped around an EGFP-VEGF-Ubx fiber (green; AVI).

Z-stack image of an endothelial sprout (blue; DAPI stained cells) passing by an EGFP-Ubx fiber (green; AVI).

AUTHOR INFORMATION

Corresponding Authors

*E-mail: kbayless@medicine.tamhsc.edu.
*E-mail: sebondos@medicine.tamhsc.edu.

Notes

The authors declare no competing financial interest.

ACKNOWLEDGMENTS

The authors would like to thank the members of the Bayless and Bondos laboratories for helpful discussions and comments on the manuscript. We would like to especially thank Colette Abbey for maintenance of ECs and Dr. Emily Wilson for the use of a National dissection scope (Model DC5-420TH). Funding was provided by NSF CAREER 1151394, the Ted Nash Long Life Foundation M1500779, and TAMHSC RDEAP to S.E.B., as well as PHS Grant HL095786 to K.J.B.

REFERENCES

(1) Marler, J. J.; Upton, J.; Langer, R.; Vacanti, J. P. Transplantation of cells in matrices for tissue regeneration. *Adv. Drug Delivery Rev.* **1998**, *33*, 165−182.

(2) Nerem, R. Cellular Engineering. *Ann. Biomed. Eng.* **1991**, *19*, 529−45.

(3) Vacanti, J. P.; Langer, R. Tissue engineering: the design and fabrication of living replacement devices for surgical reconstruction and transplantation. *Lancet* **1999**, *354*, S32−S34.

(4) Bryant, S. J.; Anseth, K. S. The effects of scaffold thickness on tissue engineered cartilage in photocrosslinked poly(ethylene oxide) hydrogels. *Biomaterials* **2001**, *22*, 619−626.

(5) Bursac, N.; Papadaki, M.; Cohen, R. J.; Schoen, F. J.; Eisenberg, S. R.; Carrier, R.; Vunjak-Novakovic, G.; Freed, L. E. Cardiac muscle tissue engineering: toward an in vitro model for electrophysiological studies. *Am. J. Physiol.* **1999**, *277*, H433−H444.

(6) Li, R. K.; Yau, T. M.; Weisel, R. D.; Mickle, D. A. G.; Sakai, T.; Choi, A.; Jia, Z. Q. Construction of a bioengineered cardiac graft. *J. Thorac. Cardiovasc. Surg.* **2000**, *119*, 368−375.

(7) Martin, I.; Vunjak-Novakovic, G.; Yang, J.; Langer, R.; Freed, L. E. Mammalian Chondrocytes Expanded in the Presence of Fibroblast Growth Factor 2 Maintain the Ability to Differentiate and Regenerate Three-Dimensional Cartilaginous Tissue. *Exp. Cell Res.* **1999**, *253*, 681−688.

(8) Obradovic, B.; Carrier, R. L.; Vunjak-Novakovic, G.; Freed, L. E. Gas exchange is essential for bioreactor cultivation of tissue engineered cartilage. *Biotechnol. Bioeng.* **1999**, *63*, 197−205.

(9) Papadaki, M.; Bursac, N.; Langer, R.; Merok, J.; Vunjak-Novakovic, G.; Freed, L. E. Tissue engineering of functional cardiac muscle: molecular, structural, and electrophysiological studies. *Am. J. Physiol.* **2001**, *280*, H168−H178.

(10) Tian, L.; George, S. C. Biomaterials to Prevascularize Engineered Tissues. *J. Cardiovasc. Transl. Res.* **2011**, *4*, 685−698.

(11) Guilak, F.; Cohen, D. M.; Estes, B. T.; Gimble, J. M.; Liedtke, W.; Chen, C. S. Control of stem cell fate by physical interactions with the extracellular matrix. *Cell stem cell* **2009**, *5*, 17−26.

(12) Hanjaya-Putra, D.; Gerecht, S. Vascular engineering using human embryonic stem cells. *Biotechnol. Prog.* **2009**, *25*, 2−9.

(13) Martino, M. M.; Brkic, S.; Bovo, E.; Burger, M.; Schaefer, D. J.; Wolff, T.; Gürke, L.; Briquez, P. S.; Larsson, H. M.; Gianni-Barrera, R.; Hubbell, J. A.; Banfi, A. Extracellular Matrix and Growth Factor Engineering for Controlled Angiogenesis in Regenerative Medicine. *Front. Bioeng. Biotechnol.* **2015**, *3*, 45.

(14) Bayless, K. J.; Davis, G. E. Sphingosine-1-phosphate markedly induces matrix metalloproteinase and integrin-dependent human endothelial cell invasion and lumen formation in three-dimensional collagen and fibrin matrices. *Biochem. Biophys. Res. Commun.* **2003**, *312*, 903−913.

(15) Carmeliet, P.; Ferreira, V.; Breier, G.; Pollefeyt, S.; Kieckens, L.; Gertsenstein, M.; Fahrig, M.; Vandenhoeck, A.; Harpal, K.; Eberhardt, C.; Declercq, C.; Pawling, J.; Moons, L.; Collen, D.; Risau, W.; Nagy, A. Abnormal blood vessel development and lethality in embryos lacking a single VEGF allele. *Nature* **1996**, *380*, 435−439.

(16) Jakeman, L.; Armanini, M.; Phillips, H.; Ferrara, N. Developmental expression of binding sites and messenger ribonucleic acid for vascular endothelial growth factor suggests a role for this

DOI: 10.1021/acs.biomac.6b01068
Biomacromolecules 2016, 17, 3558−3569

protein in vasculogenesis and angiogenesis. *Endocrinology* **1993**, *133*, 848−859.
(17) Pownall, M. E.; Isaacs, H. V. FGF Signalling in Vertebrate Development. *Coll. Series Dev. Biol.* **2010**, *1*, 1−75.
(18) Shweiki, D.; Itin, A.; Neufeld, G.; Gitay-Goren, H.; Keshet, E. Patterns of expression of vascular endothelial growth factor (VEGF) and VEGF receptors in mice suggest a role in hormonally regulated angiogenesis. *J. Clin. Invest.* **1993**, *91*, 2235−2243.
(19) Koch, S.; Claesson-Welsh, L. Signal Transduction by Vascular Endothelial Growth Factor Receptors. *Cold Spring Harbor Perspect. Med.* **2012**, *2*, a006502.
(20) Lamalice, L.; Le Boeuf, F.; Huot, J. Endothelial Cell Migration During Angiogenesis. *Circ. Res.* **2007**, *100*, 782−794.
(21) Rousseau, S.; Houle, F.; Kotanides, H.; Witte, L.; Waltenberger, J.; Landry, J.; Huot, J. Vascular Endothelial Growth Factor (VEGF)-driven Actin-based Motility Is Mediated by VEGFR2 and Requires Concerted Activation of Stress-activated Protein Kinase 2 (SAPK2/p38) and Geldanamycin-sensitive Phosphorylation of Focal Adhesion Kinase. *J. Biol. Chem.* **2000**, *275*, 10661−10672.
(22) Richardson, T. P.; Peters, M. C.; Ennett, A. B.; Mooney, D. J. Polymeric system for dual growth factor delivery. *Nat. Biotechnol.* **2001**, *19*, 1029−1034.
(23) Lee, K. Y.; Peters, M. C.; Mooney, D. J. Comparison of vascular endothelial growth factor and basic fibroblast growth factor on angiogenesis in SCID mice. *J. Controlled Release* **2003**, *87*, 49−56.
(24) Sun, G.; Shen, Y.-I.; Kusuma, S.; Fox-Talbot, K.; Steenbergen, C. J.; Gerecht, S. Functional neovascularization of biodegradable dextran hydrogels with multiple angiogenic growth factors. *Biomaterials* **2011**, *32*, 95−106.
(25) Patel, A. S.; Smith, A.; Attia, R. Q.; Mattock, K.; Humphries, J.; Lyons, O.; Saha, P.; Modarai, B.; Jayasinghe, S. N. Encapsulation of angiogenic monocytes using bio-spraying technology. *Integrative Biology* **2012**, *4*, 628−632.
(26) Hersel, U.; Dahmen, C.; Kessler, H. RGD modified polymers: biomaterials for stimulated cell adhesion and beyond. *Biomaterials* **2003**, *24*, 4385−4415.
(27) Woolfson, D. N.; Mahmoud, Z. N. More than just bare scaffolds: Towards multi-component and decorated fibrous biomaterials. *Chem. Soc. Rev.* **2010**, *39*, 3464−3479.
(28) Adak, A. K.; Li, B. Y.; Huang, L. D.; Lin, T.-W.; Chang, T. C.; Hwang, K. C.; Lin, C. C. Fabrication of Antibody Microarrays by Light-Induced Covalent and Oriented Immobilization. *ACS Appl. Mater. Interfaces* **2014**, *6*, 10452−10460.
(29) Alsop, A. T.; Pence, J. C.; Weisgerber, D. W.; Harley, B. A. C.; Bailey, R. C.; Modarai, B. Photopatterning of vascular endothelial growth factor within collagen-glycosaminoglycan scaffolds can induce a spatially confined response in human umbilical vein endothelial cells. *Acta Biomater.* **2014**, *10*, 4715−4722.
(30) Chiu, L. L. Y.; Radisic, M. Scaffolds with covalently immobilized VEGF and Angiopoietin-1 for vascularization of engineered tissues. *Biomaterials* **2010**, *31*, 226−241.
(31) Hall, H. Modified fibrin hydrogel matrices: Both, 3D-scaffolds and local and controlled release systems to stimulate angiogenesis. *Curr. Pharm. Des.* **2007**, *13*, 3597−3607.
(32) Ko, H. C. H.; Milthorpe, B. K.; McFarland, C. D. Engineering thick tissues- The vascularization problem. *Eur. Cell. Mater.* **2007**, *14*, 1−18.
(33) Köhn-Luque, A.; Back, W. D.; Yamaguchi, Y.; Yoshimura, K.; Herrero, M. A.; Miura, T. Dynamics of VEGF matrix-retention in vascular network patterning. *Phys. Biol.* **2013**, *10*, 066007−066020.
(34) Moon, J. J.; Saik, J. E.; Poche', R. A.; Leslie-Barbick, J. E.; Lee, S. H.; Smith, A. A.; Dickinson, M. E.; West, J. L. Biomimetic hydrogels with pro-angiogenic properties. *Biomaterials* **2010**, *31*, 3840−3847.
(35) Huang, Z.; Salim, T.; Brawley, A.; Patterson, J.; Matthews, K. S.; Bondos, S. E. Functionalization and patterning of protein-based materials using active ultrabithorax chimeras. *Adv. Funct. Mater.* **2011**, *21*, 2633−2640.
(36) Tsai, S. P.; Howell, D. W.; Huang, Z.; Hsiao, H.-C.; Lu, Y.; Matthews, K. S.; Lou, J.; Bondos, S. E. The Effect of Protein Fusions on the Production and Mechanical Properties of Protein-Based Materials. *Adv. Funct. Mater.* **2015**, *25*, 1442−1450.
(37) Zhang, L.; Franks, J.; Stolz, D. B.; Conway, J. F.; Thibodeau, P. H. Inducible Polymerization and Two-Dimensional Assembly of the Repeats-in-Toxin (RTX) Domain from the Pseudomonas aeruginosa Alkaline Protease. *Biochemistry* **2014**, *53*, 6452−6462.
(38) Johansson, U.; Ria, M.; Åvall, K.; Dekki Shalaly, N.; Zaitsev, S. V.; Berggren, P.-O.; Hedhammar, M. Pancreatic Islet Survival and Engraftment Is Promoted by Culture on Functionalized Spider Silk Matrices. *PLoS One* **2015**, *10*, e0130169.
(39) Zhao, W.; Han, Q.; Lin, H.; Sun, W.; Gao, Y.; Zhao, Y.; Wang, B.; Wang, X.; Chen, B.; Xiao, Z.; Dai, J. Human Basic Fibroblast Growth Factor Fused with Kringle4 Peptide Binds to a Fibrin Scaffold and Enhances Angiogenesis. *Tissue Eng., Part A* **2009**, *15*, 991−998.
(40) Yanagisawa, S.; Zhu, Z.; Kobayashi, I.; Uchino, K.; Tamada, Y.; Tamura, T.; Asakura, T. Improving Cell-Adhesive Properties of Recombinant Bombyx mori Silk by Incorporation of Collagen or Fibronectin Derived Peptides Produced by Transgenic Silkworms. *Biomacromolecules* **2007**, *8*, 3487−3492.
(41) Bini, E.; Foo, C. W. P.; Huang, J.; Karageorgiou, V.; Kitchel, B.; Kaplan, D. L. RGD-Functionalized Bioengineered Spider Dragline Silk Biomaterial. *Biomacromolecules* **2006**, *7*, 3139−3145.
(42) Jansson, R.; Thatikonda, N.; Lindberg, D.; Rising, A.; Johansson, J.; Nygren, P. Å.; Hedhammar, M. Recombinant Spider Silk Genetically Functionalized with Affinity Domains. *Biomacromolecules* **2014**, *15*, 1696−1706.
(43) Mac Gabhann, F.; Popel, A. S. Dimerization of VEGF receptors and implications for signal transduction: a computational study. *Biophys. Chem.* **2007**, *128*, 125−139.
(44) Plotnikov, A. N.; Schlessinger, J.; Hubbard, S. R.; Mohammadi, M. Structural Basis for FGF Receptor Dimerization and Activation. *Cell* **1999**, *98*, 641−650.
(45) Rodríguez-Frade, J. M.; Mellado, M.; Martínez A, C. Chemokine receptor dimerization: two are better than one. *Trends Immunol.* **2001**, *22*, 612−617.
(46) Taub, D. D. Cytokine, Growth Factor, and Chemokine Ligand Database. *Curr. Protoc. Immunol.*; John Wiley & Sons, Inc., 2001.
(47) Allen, S. J.; Crown, S. E.; Handel, T. M. Chemokine:Receptor Structure, Interactions, and Antagonism. *Annu. Rev. Immunol.* **2007**, *25*, 787−820.
(48) Kufareva, I.; Salanga, C. L.; Handel, T. M. Chemokine and chemokine receptor structure and interactions: implications for therapeutic strategies. *Immunol. Cell Biol.* **2015**, *93*, 372−383.
(49) Kufareva, I.; Salanga, C. L.; Handel, T. M. Chemokine and chemokine receptor structure and interactions: implications for therapeutic strategies. *Immunol. Cell Biol.* **2015**, *93*, 372−383.
(50) Stuttfeld, E.; Ballmer-Hofer, K. Structure and function of VEGF receptors. *IUBMB Life* **2009**, *61*, 915−922.
(51) Cabanas Danés, J. Reversibly tethering growth factors to surfaces: guiding cell function at the cell-material interface. *Ph.D. Thesis*, University of Twente, 2013
(52) Leppänen, V.-M.; Prota, A. E.; Jeltsch, M.; Anisimov, A.; Kalkkinen, N.; Strandin, T.; Lankinen, H.; Goldman, A.; Ballmer-Hofer, K.; Alitalo, K. Structural determinants of growth factor binding and specificity by VEGF receptor 2. *Proc. Natl. Acad. Sci. U. S. A.* **2010**, *107*, 2425−2430.
(53) Patterson, J. L.; Abbey, C. A.; Bayless, K. J.; Bondos, S. E. Materials composed of the Drosophila melanogaster protein ultrabithorax are cytocompatible. *J. Biomed. Mater. Res., Part A* **2014**, *102*, 97−104.
(54) Patterson, J. L.; Arenas-Gamboa, A. M.; Wang, T. Y.; Hsiao, H. C.; Howell, D. W.; Pellois, J. P.; Rice-Ficht, A.; Bondos, S. E. Materials composed of the Drosophila Hox protein Ultrabithorax are biocompatible and nonimmunogenic. *J. Biomed. Mater. Res., Part A* **2015**, *103*, 1546−1553.
(55) Greer, A. M.; Huang, Z.; Oriakhi, A.; Lu, Y.; Lou, J.; Matthews, K. S.; Bondos, S. E. The drosophila transcription factor ultrabithorax self-assembles into protein-based biomaterials with multiple morphologies. *Biomacromolecules* **2009**, *10*, 829−837.

DOI: 10.1021/acs.biomac.6b01068
Biomacromolecules 2016, 17, 3558−3569

(56) Howell, D. W.; Tsai, S. P.; Churion, K.; Patterson, J.; Abbey, C.; Porterpan, D.; You, Y. H.; Meissner, K. E.; Bayless, K. J.; Bondos, S. E. Identification of multiple dityrosine bonds in materials composed of the Drosophila protein Ultrabithorax. *Adv. Funct. Mater.* **2015**, *25*, 5988−5998.
(57) Huang, Z.; Lu, Y.; Majithia, R.; Shah, J.; Meissner, K.; Matthews, K. S.; Bondos, S. E.; Lou, J. Size dictates mechanical properties for protein fibers self-assembled by the drosophila hox transcription factor ultrabithorax. *Biomacromolecules* **2010**, *11*, 3644−3651.
(58) Bayless, K. J.; Kwak, H. I.; Su, S. C. Investigating endothelial invasion and sprouting behavior in three-dimensional collagen matrices. *Nat. Protoc.* **2009**, *4*, 1888−1898.
(59) Limaye, V.; Li, X.; Hahn, C.; Xia, P.; Berndt, M. C.; Vadas, M. A.; Gamble, J. R. Sphingosine kinase-1 enhances endothelial cell survival through a PECAM-1-dependent activation of PI-3K/Akt and regulation of Bcl-2 family members. *Blood* **2005**, *105*, 3169−3177.
(60) Dave, J. M.; Abbey, C. A.; Duran, C. L.; Seo, H.; Johnson, G. A.; Bayless, K. J. Hic-5 mediates the initiation of endothelial sprouting by regulating a key surface metalloproteinase. *J. Cell Sci.* **2016**, *129*, 743−756.
(61) Baker, M.; Robinson, S. D.; Lechertier, T.; Barber, P. R.; Tavora, B.; D'Amico, G.; Jones, D. T.; Vojnovic, B.; Hodivala-Dilke, K. Use of the mouse aortic ring assay to study angiogenesis. *Nat. Protoc.* **2011**, *7*, 89−104.
(62) Dohle, D. S.; Pasa, S. D.; Gustmann, S.; Laub, M.; Wissler, J. H.; Jennissen, H. P.; Dünker, N. Chick ex ovo Culture and ex ovo CAM Assay: How it Really Works. *J. Visualized Exp.* **2009**, *33*, 1620−1626.
(63) Bayless, K. J.; Davis, G. E. Microtubule Depolymerization Rapidly Collapses Capillary Tube Networks in Vitro and Angiogenic Vessels in Vivo through the Small GTPase Rho. *J. Biol. Chem.* **2004**, *279*, 11686−11695.
(64) Sys, G. M. L.; Lapeire, L.; Stevens, N.; Favoreel, H.; Forsyth, R.; Bracke, M.; De Wever, O. The In ovo CAM-assay as a Xenograft Model for Sarcoma. *J. Visualized Exp.* **2013**, *77*, 50522−50529.
(65) Dougher, M.; Terman, B. I. Autophosphorylation of KDR in the kinase domain is required for maximal VEGF-stimulated kinase activity and receptor internalization. *Oncogene* **1999**, *18*, 1619−1627.
(66) Kendall, R. L.; Rutledge, R. Z.; Mao, X.; Tebben, A. J.; Hungate, R. W.; Thomas, K. A. Vascular endothelial growth factor receptor KDR tyrosine kinase activity is increased by autophosphorylation of two activation loop tyrosine residues. *J. Biol. Chem.* **1999**, *274*, 6453−6460.
(67) Matsumoto, T.; Bohman, S.; Dixelius, J.; Berge, T.; Dimberg, A.; Magnusson, P.; Wang, L.; Wikner, C.; Qi, J. H.; Wernstedt, C.; Wu, J.; Bruheim, S.; Mugishima, H.; Mukhopadhyay, D.; Spurkland, A.; Claesson-Welsh, L. VEGF receptor-2 Y951 signaling and a role for the adapter molecule TSAd in tumor angiogenesis. *EMBO J.* **2005**, *24*, 2342−2353.
(68) Matsumoto, T.; Claesson-Welsh, L. VEGF receptor signal transduction. *Sci. Signaling* **2001**, *2001*, re21−39.
(69) Plouët, J.; Moukadiri, H. Characterization of the receptor to vasculotropin on bovine adrenal cortex-derived capillary endothelial cells. *J. Biol. Chem.* **1990**, *265*, 22071−22074.
(70) Terman, B. I.; Carrion, M. E.; Kovacs, E.; Rasmussen, B. A.; Eddy, R. L.; Shows, T. B. Identification of a new endothelial cell growth factor receptor tyrosine kinase. *Oncogene* **1991**, *6*, 1677−1683.
(71) Vaisman, N.; Gospodarowicz, D.; Neufeld, G. Characterization of the receptors for vascular endothelial growth factor. *J. Biol. Chem.* **1990**, *265*, 19461−19466.
(72) Dent, P. Crosstalk between ERK, AKT, and cell survival. *Cancer Biol. Ther.* **2014**, *15*, 245−246.
(73) Shu, X.; Wu, W.; Mosteller, R. D.; Broek, D. Sphingosine Kinase Mediates Vascular Endothelial Growth Factor-Induced Activation of Ras and Mitogen-Activated Protein Kinases. *Mol. Cell. Biol.* **2002**, *22*, 7758−7768.
(74) Zachary, I. VEGF signalling: integration and multi-tasking in endothelial cell biology. *Biochem. Soc. Trans.* **2003**, *31*, 1171−1177.
(75) Cunningham, S. A.; Waxham, M. N.; Arrate, P. M.; Brock, T. A. Interaction of the Flt-1 tyrosine kinase receptor with the p85 subunit of phosphatidylinositol 3-kinase: Mapping of a novel site involved in binding. *J. Biol. Chem.* **1995**, *270*, 20254−20257.
(76) Gerber, H. P.; McMurtrey, A.; Kowalski, J.; Yan, M.; Keyt, B. A.; Dixit, V.; Ferrara, N. Vascular endothelial growth factor regulates endothelial cell survival through the phosphatidylinositol 3′-kinase/Akt signal transduction pathway: Requirement for Flk-1/KDR activation. *J. Biol. Chem.* **1998**, *273*, 30336−30343.
(77) Kroll, J.; Waltenberger, J. The Vascular Endothelial Growth Factor Receptor KDR Activates Multiple Signal Transduction Pathways in Porcine Aortic Endothelial Cells. *J. Biol. Chem.* **1997**, *272*, 32521−32527.
(78) Waltenberger, J.; Claesson-Welsh, L.; Siegbahn, A.; Shibuya, M.; Heldin, C. H. Different signal transduction properties of KDR and Flt1, two receptors for vascular endothelial growth factor. *J. Biol. Chem.* **1994**, *269*, 26988−26995.
(79) Silva, E. A.; Mooney, D. J. Effects of VEGF Temporal and Spatial Presentation on Angiogenesis. *Biomaterials* **2010**, *31*, 1235.
(80) Christenson, L. K.; Stouffer, R. L. Isolation and culture of microvascular endothelial cells from the primate corpus luteum. *Biol. Reprod.* **1996**, *55*, 1397−1404.
(81) Hermann, D. M.; Zechariah, A. Implications of vascular endothelial growth factor for postischemic neurovascular remodeling. *J. Cereb. Blood Flow Metab.* **2009**, *29*, 1620−1643.
(82) Breslin, J. W.; Pappas, P. J.; Cerveira, J. J.; Hobson, R. W.; Durán, W. N. VEGF increases endothelial permeability by separate signaling pathways involving ERK-1/2 and nitric oxide. *Am. J. Physiol. Heart Circ. Physiol.* **2003**, *284*, H92−H100.
(83) Fujioka, A.; Terai, K.; Itoh, R. E.; Aoki, K.; Nakamura, T.; Kuroda, S.; Nishida, E.; Matsuda, M. Dynamics of the Ras/ERK MAPK Cascade as Monitored by Fluorescent Probes. *J. Biol. Chem.* **2006**, *281*, 8917−8926.
(84) Anderson, S. M.; Chen, T. T.; Iruela-Arispe, M. L.; Segura, T. The phosphorylation of vascular endothelial growth factor receptor-2 (VEGFR-2) by engineered surfaces with electrostatically or covalently immobilized VEGF. *Biomaterials* **2009**, *30*, 4618−4628.
(85) Anderson, S. M.; Shergill, B.; Barry, Z. T.; Manousiouthakis, E.; Chen, T. T.; Botvinick, E.; Platt, M. O.; Iruela-Arispe, M. L.; Segura, T. VEGF internalization is not required for VEGFR-2 phosphorylation in bioengineered surfaces with covalently linked VEGF. *Integr. Biol.* **2011**, *3*, 887−896.
(86) Anderson, S. M.; Siegman, S. N.; Segura, T. The effect of vascular endothelial growth factor (VEGF) presentation within fibrin matrices on endothelial cell branching. *Biomaterials* **2011**, *32*, 7432−7443.
(87) Shen, Y. H.; Shoichet, M. S.; Radisic, M. Vascular endothelial growth factor immobilized in collagen scaffold promotes penetration and proliferation of endothelial cells. *Acta Biomater.* **2008**, *4*, 477−489.
(88) Pitulescu, M. E.; Adams, R. H. Regulation of signaling interactions and receptor endocytosis in growing blood vessels. *Cell Adh. Migr.* **2014**, *8*, 366−377.
(89) Heintz, K. A.; Bregenzer, M. E.; Mantle, J. L.; Lee, K. H.; West, J. L.; Slater, J. H. Fabrication of 3D Biomimetic Microfluidic Networks in Hydrogels. *Adv. Healthcare Mater.* **2016**, *5*, 2153−2160.
(90) Park, J. Y.; Shim, J.-H.; Choi, S.-A.; Jang, J.; Kim, M.; Lee, S. H.; Cho, D.-W. 3D printing technology to control BMP-2 and VEGF delivery spatially and temporally to promote large-volume bone regeneration. *J. Mater. Chem. B* **2015**, *3*, 5415−5425.
(91) Miyagi, Y.; Chiu, L. L. Y.; Cimini, M.; Weisel, R. D.; Radisic, M.; Li, R. K. Biodegradable collagen patch with covalently immobilized VEGF for myocardial repair. *Biomaterials* **2011**, *32*, 1280−1290.
(92) Zieris, A.; Prokoph, S.; Levental, K. R.; Welzel, P. B.; Grimmer, M.; Freudenberg, U.; Werner, C. FGF-2 and VEGF functionalization of starPEG−heparin hydrogels to modulate biomolecular and physical cues of angiogenesis. *Biomaterials* **2010**, *31*, 7985−7994.
(93) Murschel, F.; Liberelle, B.; St-Laurent, G.; Jolicoeur, M.; Durocher, Y.; De Crescenzo, G. Coiled-coil-mediated grafting of bioactive vascular endothelial growth factor. *Acta Biomater.* **2013**, *9*, 6806−6813.

DOI: 10.1021/acs.biomac.6b01068
Biomacromolecules 2016, 17, 3558−3569

(94) Aizawa, Y.; Wylie, R.; Shoichet, M. Endothelial Cell Guidance in 3D Patterned Scaffolds. *Adv. Mater.* **2010**, *22*, 4831−4835.
(95) He, Q.; Zhao, Y.; Chen, B.; Xiao, Z.; Zhang, J.; Chen, L.; Chen, W.; Deng, F.; Dai, J. Improved cellularization and angiogenesis using collagen scaffolds chemically conjugated with vascular endothelial growth factor. *Acta Biomater.* **2011**, *7*, 1084−1093.
(96) Wang, A. Y.; Leong, S.; Liang, Y. C.; Huang, R. C. C.; Chen, C. S.; Yu, S. M. Immobilization of Growth Factors on Collagen Scaffolds Mediated by Polyanionic Collagen Mimetic Peptides and Its Effect on Endothelial Cell Morphogenesis. *Biomacromolecules* **2008**, *9*, 2929−2936.
(97) Ozawa, C. R.; Banfi, A.; Glazer, N. L.; Thurston, G.; Springer, M. L.; Kraft, P. E.; McDonald, D. M.; Blau, H. M. Microenvironmental VEGF concentration, not total dose, determines a threshold between normal and aberrant angiogenesis. *J. Clin. Invest.* **2004**, *113*, 516−527.
(98) Yang, J.; Li, W.; He, X.; Zhang, G.; Yue, L.; Chai, Y. VEGF Overexpression Is a Valuable Prognostic Factor for Non-Hodgkin's Lymphoma Evidence from a Systemic Meta-Analysis. *Dis. Markers* **2015**, *2015*, 786790−786799.
(99) Appelmann, I.; Liersch, R.; Kessler, T.; Mesters, R.; Berdel, W. Angiogenesis Inhibition in Cancer Therapy. *Recent Results Cancer Res.* **2010**, *180*, 51−81.
(100) Ellis, L. M.; Hicklin, D. J. VEGF-targeted therapy: mechanisms of anti-tumour activity. *Nat. Rev. Cancer* **2008**, *8*, 579−591.
(101) Olsson, A. K.; Dimberg, A.; Kreuger, J.; Claesson-Welsh, L. VEGF receptor signalling ? in control of vascular function. *Nat. Rev. Mol. Cell Biol.* **2006**, *7*, 359−371.
(102) Farahani, M.; Treweeke, A. T.; Toh, C. H.; Till, K. J.; Harris, R. J.; Cawley, J. C.; Zuzel, M.; Chen, H. Autocrine VEGF mediates the antiapoptotic effect of CD154 on CLL cells. *Leukemia* **2005**, *19*, 524−530.
(103) Yang, Z.; Mo, X.; Gong, Q.; Pan, Q.; Yang, X.; Cai, W.; Li, C.; Ma, J. X.; He, Y.; Gao, G. Critical effect of VEGF in the process of endothelial cell apoptosis induced by high glucose. *Apoptosis* **2008**, *13*, 1331−1343.
(104) Roberts, J. R.; Perkins, G. D.; Fujisawa, T.; Pettigrew, K. A.; Gao, F.; Ahmed, A.; Thickett, D. R. Vascular endothelial growth factor promotes physical wound repair and is anti-apoptotic in primary distal lung epithelial and A549 cells. *Crit. Care Med.* **2007**, *35*, 2164−2170.
(105) Masson, V.; Devy, L.; Grignet-Debrus, C.; Bernt, S.; Bajou, K.; Blacher, S.; Roland, G.; Chang, Y.; Fong, T.; Carmeliet, P.; Foidart, J. M.; Noël, A. Mouse Aortic Ring Assay: A New Approach of the Molecular Genetics of Angiogenesis. *Biol. Proced. Online* **2002**, *4*, 24−31.

DOI: 10.1021/acs.biomac.6b01068
Biomacromolecules 2016, 17, 3558−3569

Supporting Information

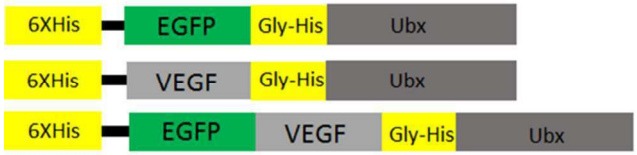

Supporting Information Figure 1. Schematic of Ubx fusions.

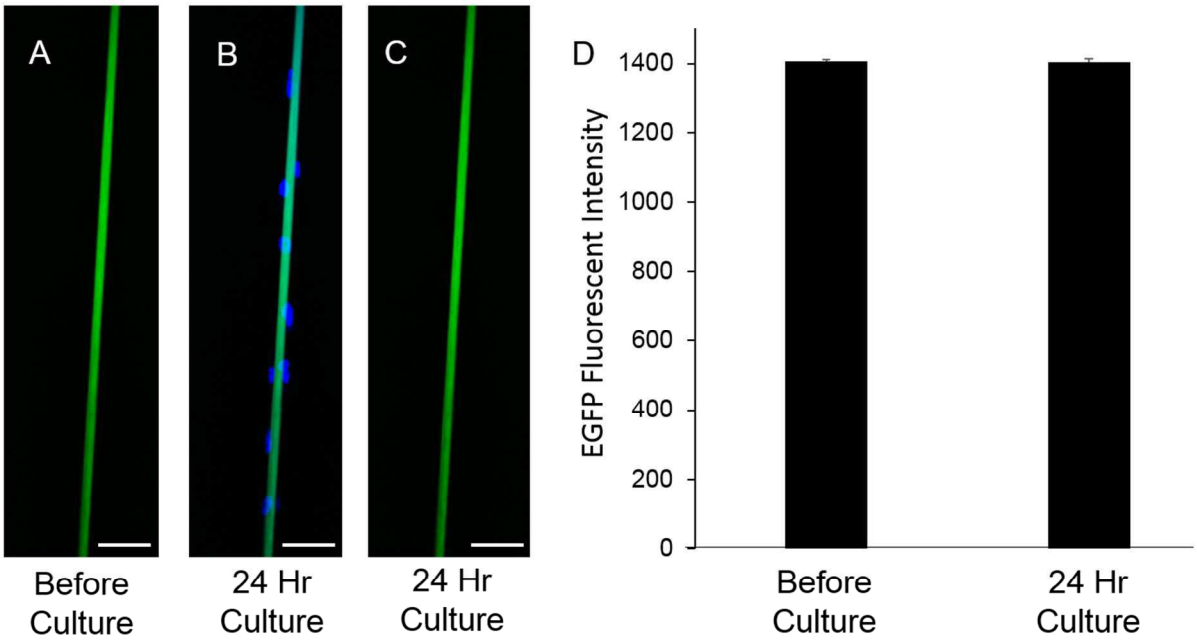

Supporting Information 2. EGFP is not released from EGFP-VEGF-Ubx fibers when cultured with endothelial cells. EGFP-VEGF-Ubx fibers imaged using confocal microscopy (A) before and (B,C) 24 hours after cell culture. (B) Green Channel only. (C) Green and Blue channel showing DAPI stained cells. Scale bars equal 50 μm. Identical coordinates where imaged in panels A-C. (D) EGFP fluorescent intensity quantification (3 samples; 25 replicates) shows that there is no difference between fibers before and after culture. EGFP is tethered to Ubx materials via VEGF (Figure S1), if VEGF were degraded by cell culture then EGFP would be lost from the fiber. Since there is no difference in EGFP intensity, we can assume that VEGF is at least intact.

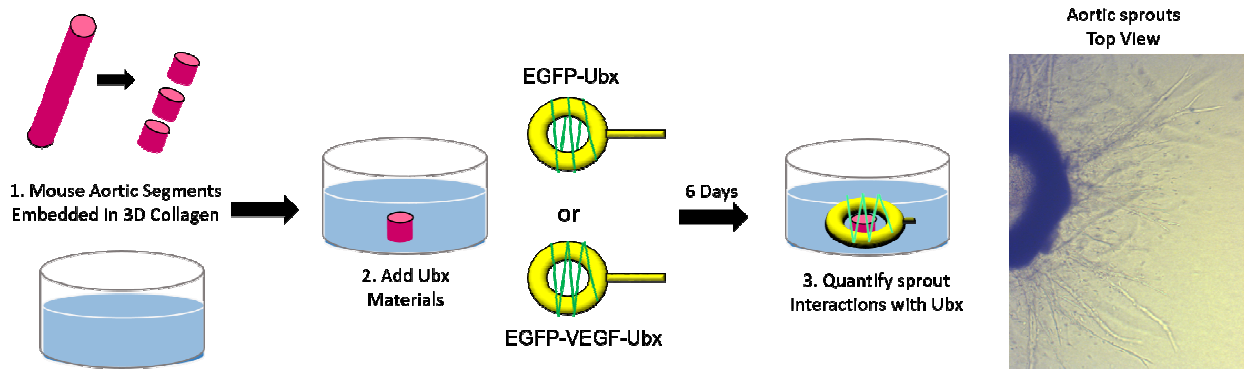

Supporting Information 3. Schematic of modification of mouse aortic ring assay for use with Ubx materials. Note that sprouts emanate linearly from tissue radius.

Supporting Information Figure 4. Z-stack image of an endothelial sprout (blue; DAPI stained cells) wrapped around an EGFP-VEGF-Ubx fiber (green).

Supporting Information Figure 5. Z-stack image of an endothelial sprout (blue; DAPI stained cells) passing by an EGFP-Ubx fiber (green).